

UC Irvine

UC Irvine Previously Published Works

Title

Characterizing tourniquet induced hemodynamics during total knee arthroplasty using diffuse optical spectroscopy

Permalink

<https://escholarship.org/uc/item/6p44p0w5>

Journal

Journal of Orthopaedic Research®, 41(1)

ISSN

0736-0266

Authors

Philipopoulos, George P
Sharareh, Behnam
Ganesan, Goutham
[et al.](#)

Publication Date

2023

DOI

10.1002/jor.25327

Peer reviewed

Ran Schwarzkopf ORCID iD: 0000-0003-0681-7014

**Characterizing tourniquet induced hemodynamics during total knee arthroplasty
using diffuse optical spectroscopy**

George P. Philipopoulos¹, Behnam Sharareh², Goutham Ganesan^{1,3}, Bruce J. Tromberg¹,
Thomas D. O'Sullivan⁴, and Ran Schwarzkopf⁵

¹University of California, Irvine, Beckman Laser Institute and Medical Clinic, Laser
Microbeam and Medical Program, 1002 Health Sciences Road, Irvine, CA 92617, USA

²University of Washington, Department of Orthopaedics and Sport Medicine, Seattle,
WA, USA

³University of California Irvine, Institute for Clinical and Translation Science, 843
Hewitt Hall, Irvine, USA, 92617

⁴University of Notre Dame, Department of Electrical Engineering, 275 Fitzpatrick Hall,
Notre Dame, IN 46556 USA

⁵NYU Langone Orthopaedic Hospital, Hospital for Joint Diseases, 301 East 17th Street,
New York, NY 10003 USA

Corresponding author: Ran Schwarzkopf; schwarzk@gmail.com

Running Title: Optics for tourniquet induced hemodynamics

Author Contributions: BJT, TDO and RS contributed to the research design. GP, BS and

GG acquired data. GP, GG, BJT and TDO analyzed and interpreted the results. GP and

BS wrote the manuscript with critical revisions from TDO, GG, BJT, and RS. All authors

have read and approved the final submitted manuscript.

Abstract:

Tourniquet use creates a reduced blood surgical field during total knee arthroplasty

(TKA), however, prolonged ischemia may cause post-operative tourniquet complications.

This article has been accepted for publication and undergone full peer review but has not
been through the copyediting, typesetting, pagination and proofreading process, which
may lead to differences between this version and the Version of Record. Please cite this
article as doi: 10.1002/jor.25327.

This article is protected by copyright. All rights reserved.

To understand the effects of tourniquet-induced ischemia, we performed a prospective observational study using quantitative broadband diffuse optical spectroscopy (DOS) to measure tissue hemodynamics and water and lipid concentrations before, during, and after tourniquet placement in subjects undergoing TKA. Data was collected for six months and, of the total subjects analyzed (n=24), 22 were primary TKAs and 2 were revision TKA cases. We specifically investigated tourniquet-induced hemodynamics based upon subject-specific tissue composition and observed a significant relationship between the linear rate of deoxygenation after tourniquet inflation and water/lipid ratio (W/L, $p < 0.0001$) and baseline somatic tissue oxygen saturation, StO_2 ($p = 0.05$). Subjects with a low W/L ratio exhibited a lower tissue metabolic rate of oxygen consumption, $tMRO_2$ ($p = 0.008$). Changes in deoxyhemoglobin [HbR] ($p = 0.009$) and lipid fraction ($p = 0.001$) were significantly different between high and low W/L subject groups during deoxygenation. No significant differences were observed for hemodynamics during reperfusion and total tourniquet time was neither significantly related to the hemodynamic hyperemic response ($p = 0.73$) nor the time to max StO_2 after tourniquet release ($p = 0.57$). In conclusion, we demonstrate that DOS is capable of real-time monitoring of tissue hemodynamics distal to the tourniquet during TKA, and that tissue composition should be considered. DOS may help surgeons stratify hemodynamics based upon tissue composition and eventually aid the pre-operative risk assessment of vascular occlusions from tourniquet use during TKA.

Keywords: diffuse optics, noninvasive, orthopaedic surgery, reactive hyperemia, spectroscopy, tissue oxygen saturation

1. Introduction

During total knee arthroplasty (TKA), tourniquets are applied to create a reduced blood surgical field [1-3]. Benefits of tourniquet use include decreased intraoperative blood loss and overall reduced operative time [4-6]. However, it has also been shown that prolonged ischemia distal to the tourniquet may lead to muscle weakness, vascular injury, and increased post-operative pain [7]. These negative consequences are associated with the duration of inflation suggesting the importance of monitoring tissue hemodynamics before, during, and after tourniquet placement [4-6].

Near-infrared spectroscopy (NIRS) is an optical method that can noninvasively characterize deep tissue hemoglobin oxygen saturation of arterial, capillary and venous blood volumes. Previously, NIRS has proven useful in the orthopaedic clinical setting when monitoring tourniquet assisted procedures [8-10]. Shadgan et al. monitored the hemodynamics of the tibialis anterior muscle during ankle fracture repair surgery. This study found negative correlations between tourniquet induced muscle damage and local tissue changes of NIRS measured total- and oxy-hemoglobin [9], suggesting that muscle damage distal to tourniquet application may be assessed using NIRS. A similar study by Lin et al., wherein NIRS was applied continuously to monitor tissue oxygenation both distal and proximal to tourniquet application during ankle surgery [8]. However, they noted that tissue desaturation after tourniquet inflation was highly variable and suggested this may be due to inter-subject differences in skin and subcutaneous adipose tissue thickness. Indeed, a limitation of NIRS is the commonly invoked assumption that tissue is homogeneous [11, 12]. This restricts the ability of NIRS to separate signal contributions from multiple layers of tissue [13-16]. When using NIRS to measure muscle oxygenation, measurement sensitivity and accuracy are greatly affected by the

subcutaneous layer which varies between individuals based on adipose tissue thickness [14]. Continuous-wave (CW)-NIRS, the technique used in these studies to date, only monitors relative changes in hemoglobin levels and is unable to quantify absolute tissue, such as the subcutaneous water and lipid content.

In this study, we apply a lab-developed hybrid diffuse optical spectroscopy (DOS) instrument that utilizes a combination of broadband CW and frequency-domain NIRS to quantify hemodynamics and tissue water and lipid composition distal to tourniquet application during total knee arthroplasty [17-19]. Unlike typical tissue oximeters which use CW- only, a key feature of this broadband technique is its ability to directly measure tissue optical properties. This allows for the absolute measurement of oxyhemoglobin [HbO₂], deoxyhemoglobin [HbR], water, lipid, and tissue optical scattering parameters [17-20]. Together, these parameters represent structural and molecular information about tissue, indirectly reflecting metabolism, perfusion, hydration and total blood volume [21-23].

The purpose of this study was to investigate the intraoperative use of DOS during TKA and characterize tourniquet-induced hemodynamics based upon subject-specific tissue composition, using a DOS derived W/L ratio. We hypothesized that this quantitative sensing approach is sensitive to disparate hemodynamic profiles between tissue composition types [24-26], which are important for establishing normative measures in relation to patient pain [27], muscle damage [9], and post-operative recovery [28, 29]. Therefore, using DOS in this clinical application is especially relevant given the patient populations undergoing these procedures often have cardiovascular comorbidities which affect pre-operative risk stratification.

2. Methods

2.1 Subject Population

This prospective observational study was approved by our Institutional Review Board and all subjects provided written informed consent. Designed as a pilot feasibility study, lower extremity tissue oxygenation was monitored in 34 subjects undergoing total knee arthroplasty under general (n=14) and spinal (n=20) anesthesia. 27 subjects were primary TKAs and 7 were revision TKA cases. All cases were done through a medial parapatellar approach. Knee flexion was used for most of the bony preparation except during patellar resurfacing, balancing, and cement hardening. The surgical technique was not changed or adjusted for the research study. DOS signal to noise ratio (SNR) was calculated for each case based on the detected optical signal amplitude at each laser diode compared to a prior measurement of the instrument noise floor. Subjects that did not meet a minimum threshold for DOS (SNR) were excluded from the study. Low SNR was primarily due to poor optical coupling between the tissue probe and the DOS instrument itself (n=3) and high attenuation due to absorption and scattering of tissue (n=2), which was dependent on the subject. Additional reasons for exclusion included instrument failure (n=3), inconsistent tourniquet pressure (n=1), and failed instrument calibration (n=1). A total of 24 subjects (13 female, 11 male) were analyzable and included in the study. A direct comparison between primary (n=22) and revision TKA (n=2) cases was not possible due to the small sample size in revision cases. Of the 24 subjects, tourniquet pressure was set at 250 mmHg, consistent with the standard-of-care for this procedure. The tourniquet pressure was not adjusted based on the subject's blood pressure. Additional subject demographics recorded during this study included age, ethnicity, body mass index,

height, and weight. In addition, comorbidities were documented. Subject demographics and tourniquet inflation time are summarized in table 1.

2.2 DOS Instrumentation

Tissue oxygenation was monitored with a fiber-coupled optical probe with a 20 mm source-detector separation placed 2 cm distal to a non-sterile tourniquet on the operated limb over the quadriceps muscle, outside of the sterile surgical field, prior to surgical draping. After the probe was secured, measurements were taken continuously at 15 sec intervals. Measurements were concluded just before wound closure was initiated, which was defined as the end of the case. Tourniquet was inflated prior to incision and was deflated prior to arthrotomy closure after the final implants were placed and the cement had fully hardened. Measurements were taken for an average of 13.8 +/- 1.9 min prior to tourniquet inflation and 34.4 +/- 17.1 min after tourniquet deflation. Figure 1 shows an example case of how the probe was placed and secured. The broadband DOS instrument used during the study was conceived and manufactured by researchers at the Beckman Laser Institute (University of California, Irvine, USA). The instrument, called a miniature diffuse optical spectroscopic imager (mDOSI), performs quantitative tissue absorption and scattering spectroscopy by combining laser-based frequency domain (FD) photon migration (658, 688, 783, 828 nm) with broadband (650-1000nm) continuous wave (CW) reflectance spectroscopy. Details of the combined CW and FD DOS technique have been previously described [17]. Briefly, tissue absorption (μ_a) and reduced scattering (μ'_s) coefficients were derived from DOS data using model-based fitting. Broadband tissue optical scattering was estimated from FD-measured reduced scattering using the equation $\mu'_s = A(\lambda/\lambda_0)^{-b}$, and used to extract absolute tissue absorption from the CW reflectance. Scattering prefactor (A) and scattering power (b) represent reduced scattering coefficient

at $\lambda_0 = 500$ nm and wavelength dependence of scattering, respectively. Both parameters are reflective of microscopic structures such as collagen and mitochondria [30]. DOS noninvasively quantifies absolute bulk tissue concentrations of oxyhemoglobin [HbO₂], deoxyhemoglobin [HbR], water, and lipid [17]. Somatic tissue oxygen saturation, StO₂ is defined as $[\text{HbO}_2]/([\text{HbO}_2] + [\text{HbR}])$ and total hemoglobin, [THb] is $[\text{HbO}_2] + [\text{HbR}]$.

2.3 Data Analysis

All data was processed in MATLAB (Mathworks, MA USA). Baseline values were calculated as the mean of 3 min of data prior to tourniquet inflation and recorded for StO₂, [HbO₂], [HbR], [THb], water and lipid. A unitless water to lipid (W/L) ratio was calculated from the baseline water and lipid composition to classify tissue composition. To visualize the influence of tissue composition on chromophore changes during deoxygenation and reperfusion, two cohorts were created differentiated by the median baseline W/L for all analyzed subjects: high ($W/L \geq 0.35$, $n=12$) and low ($W/L < 0.35$, $n=12$).

The occlusion was analyzed in two separate phases, the deoxygenation and reperfusion phase. During the deoxygenation phase, the shape language modeling tool (<http://www.mathworks.com/matlabcentral/fileexchange/24443>) was used to apply a linear piecewise fit function during the occlusion [31]. This fitting method estimates the temporal breakpoint between the rapid declining deoxygenation phase and steady-state ischemia after tourniquet inflation, assuming first-order kinetics during the deoxygenation phase. Output variables included a first phase duration time (time between tourniquet inflation and ischemia breakpoint), breakpoint StO₂ (%), and a goodness of fit metric (r-squared value). Figure 2a shows the first phase duration time representing the rapid deoxygenation phase. Other variables of interest during deoxygenation included a

linear rate of deoxygenation (%/min). This was calculated as the rate of change in StO_2 during the rapid deoxygenation phase.

The tissue metabolic rate of oxygen consumption ($tMRO_2$) was estimated from the initial changes in [HbR] after tourniquet inflation by fitting a linear regression line between 0.5 minutes after tourniquet inflation up until steady-state ischemia was achieved, determined by the temporal breakpoint. It is at this point when further [HbO₂] decline is not detected and equilibrium with oxygen delivery is achieved [32, 33]. Therefore, this time window was selected for analysis to represent the entire period of tissue oxygen consumption as a result of tourniquet application. To estimate $tMRO_2$, [HbR] changes were multiplied by 4 to accommodate for the four oxygen molecules per hemoglobin. A goodness of fit metric (r-squared value) was calculated for $tMRO_2$. Figure 2b shows a sample case representing the $tMRO_2$ fitting metric used in this study.

During reperfusion, the post-occlusion max StO_2 was identified. The hemodynamic hyperemic response, HHR (%) was quantified by subtracting the baseline StO_2 from the post-occlusion maximum StO_2 . The time-to-peak, the time after tourniquet release to reach max StO_2 , was also measured and represented as T_{peak} . A sample case dynamic and the fitting metrics used for analysis can be seen in figure 2a.

DOS parameters (StO_2 , [HbO₂], [HbR], [THb], water, lipid and W/L ratio) were recorded during deoxygenation and reperfusion for both high and low W/L subject groups to account for inter-subject variability in baseline.

2.4 Statistics

Statistical tests were completed using IBM SPSS Statistics Software (IBM, NY USA). Descriptive statistics, including mean and standard error were calculated for all subjects and measured baseline chromophore values. A multivariable linear regression

test was performed to include the effects for age, BMI, gender, baseline StO₂, and baseline THb. Comorbidities were not included in multivariable analysis due to small sample size for each individual comorbidity. Both 95% confidence intervals (CI) and beta coefficients (β) were calculated. β reflects the change in hemodynamic output variables by a single unit in W/L.

Analysis of variance (ANOVA) for repeated measures was used to determine the relationship between W/L ratio and DOS chromophore changes (StO₂, [HbO₂], [HbR], [THb], water, lipid, and W/L ratio). This was done to assess the predictability of chromophore changes based on the interaction of W/L and time with subject as a random effect to account for multiple measurements. Significance was determined by $p < 0.05$.

3. Results

3.1 Baseline Values

A total of twenty-four subjects undergoing TKA (13 female, 11 male) were analyzed for this study. The average age for study participants was 63.5 +/- 12.5 (mean +/- standard deviation) years old. Additional demographics recorded included: height (170.8 +/- 11.2 cm), weight (88.5 +/- 20.7 kg), BMI (30.5 +/- 6.7 kg/m²), and ethnicity (Caucasian, n=17, Hispanic, n= 6, Asian, n=1). Comorbidities and subject demographics are summarized in table 1. The mean baseline StO₂ for all subjects (mean +/- standard error) prior to tourniquet inflation was 70.1 +/- 2.1%. Average baseline values for the hemodynamic parameters HbO₂, HbR, and THb were 25 +/- 2.0, 9.7 +/- 0.5, and 34.7 +/- 2.1 μ M, respectively. Using a linear regression analysis, we observed a significant relationship between W/L and baseline THb ($p=0.02$, $r=0.46$). Also, there was a borderline significant relationship between W/L and baseline HbO₂ ($p=0.06$, $r=0.39$). However, no significance was observed between W/L and the following DOS

parameters: StO_2 ($p=0.61$, $r=0.11$) and HbR ($p=0.18$, $r=0.29$). Baseline values for all DOS hemodynamic parameters and correlations with W/L are summarized in table 2.

3.2 Deoxygenation Phase

The mean first phase duration time, the time it took StO_2 to reach a minimum value during tourniquet inflation for all subjects, was 25.5 ± 2.7 min. The linear rate of deoxygenation (i.e., change in StO_2) was $-1.4 \pm 0.1\%$ min. For all subjects, linear fits to determine the rates of deoxygenation were associated with a mean r-squared value of 0.831. The mean minimum StO_2 during tourniquet inflation for all subjects was $40.2 \pm 1.9\%$. For low and high W/L subject groups, the minimum StO_2 was $39.0 \pm 2.7\%$ and $41.4 \pm 2.7\%$, respectively.

A linear regression was calculated for the changes in $[HbR]$ during the first phase deoxygenation period to estimate $tMRO_2$. For all subjects, the mean $tMRO_2$ was 0.41 ± 0.08 $\mu M/sec$. Linear regression to $[HbR]$ curves during deoxygenation had a mean r-squared of 0.888. A multivariable regression analysis to include gender, age, BMI, baseline StO_2 and THb was performed to determine the relationship between the subjects' W/L ratio and hemodynamic parameters (table 3). We observed a significant relationship between W/L and the following parameters: linear rate of deoxygenation ($p<0.0001$) and $tMRO_2$ ($p=0.008$). There was a positive relationship between baseline StO_2 and the first phase duration time ($p<0.001$), showing that tissue with higher oxygen saturation took longer to deoxygenate as expected.

During deoxygenation, StO_2 and $[HbO_2]$ decreased with time in both subject groups. However, the relationship between W/L and the changes in both StO_2 and $[HbO_2]$ was not significant. The opposite trend was observed for $[HbR]$. Subjects with a greater W/L ratio demonstrated a significantly larger change in $[HbR]$ during the first 50 minutes of

deoxygenation ($p=0.009$). Figure 3 shows the observed changes over time for StO_2 , $[HbO_2]$, and $[HbR]$. $[THb]$ decreased immediately after tourniquet inflation in both subject groups. However, this change in $[THb]$ was relatively small and most likely the result of blood redistribution within the sampled tissue.

DOS chromophore changes (StO_2 , $[HbO_2]$, $[HbR]$, $[THb]$, water, lipid and W/L ratio) during deoxygenation for high and low W/L subject groups are summarized in figure 3. The measured water fraction decreased over time in both the high and low W/L ratio subject groups, which could also be related to blood redistribution. Unexpectedly, subjects with a high W/L ratio showed a decrease in lipid fraction during the first 50 minutes of deoxygenation ($p=0.001$). In contrast, subjects with increased probed adipose tissue, as indicated by a low W/L ratio had a relatively constant lipid fraction during deoxygenation. These changes were also represented in the W/L ratio changes over time.

3.3 Reperfusion Phase

18 of 24 subjects exhibited a hemodynamic hyperemic response (HHR), defined as a post-occlusive maximum StO_2 higher than baseline. Figure 2a shows a representative individual StO_2 dynamic wherein, after the tourniquet was released, StO_2 recovered and typically overshoot the baseline value demonstrating an HHR. The mean maximum StO_2 following tourniquet release was $75.5 \pm 1.4\%$, which was $5.4 \pm 1.8\%$ above baseline. The average time it took to reach max StO_2 after tourniquet release, T_{peak} , was 6.7 ± 0.5 min. No significant correlations were found between the total tourniquet time and hemodynamic parameters during the reperfusion phase: HHR ($p=0.73$) and T_{peak} ($p=0.57$). However, a significant relationship was observed between the extent of the subjects' hyperemic response and two baseline DOS parameters: StO_2 ($p<0.001$), $[THb]$ ($p=0.008$), shown in figure 4.

During the first 10 minutes of reperfusion, subjects with a lower W/L ratio exhibited a smaller change in lipid fraction over time. There was an unexpected shape observed for lipid changes in subjects with greater muscle concentration, as seen in figure 5f. DOS chromophore changes (StO_2 , $[\text{HbO}_2]$, $[\text{HbR}]$, $[\text{THb}]$, water, lipid and W/L ratio) in each subject group are summarized in figure 5.

4. Discussion

In this study, we applied a broadband, quantitative DOS sensing technique within the orthopaedic operative setting to quantify hemodynamics in ischemic tissue distal to tourniquet application during total knee arthroplasty. Hemodynamics were recorded in real-time before, during, and after tourniquet inflation. Unique to this approach compared to traditional NIRS, we also quantified water and lipid tissue concentrations. This enabled us to derive a water/lipid (W/L) ratio to assess relative amounts of “lean tissue” measured within each subject in order to get a more accurate estimation of the probed tissue depth. Moreover, this allowed us to characterize how hemodynamic profiles differ based upon tissue composition, as in the stratification of subjects based on W/L. Our multivariable analysis indicated a significant relationship between W/L and two hemodynamic parameters reflecting tissue metabolism – the linear rate of deoxygenation and tissue metabolic rate of oxygenation (tMRO_2). In addition, high and low W/L subject groups had significantly different hemodynamic profiles in deoxyhemoglobin and lipid during deoxygenation.

In all subjects undergoing TKA, subjects with a greater amount of probed adipose, as reflected by a lower W/L ratio, had a significantly slower linear rate of deoxygenation and smaller tMRO_2 than subjects with a high W/L ratio. Additionally, high and low W/L subject groups had significantly different changes in HbR during

deoxygenation. Previously, NIRS has been used to monitor muscle hemodynamics and assess microvascular changes in skeletal muscle during tourniquet assisted orthopaedic surgery. For example, Shadgan et al. demonstrated that greater changes in local oxygenated blood volume, distal to the tourniquet resulted in a lesser degree of muscle damage during ankle fracture repair surgery [9]. However, due to tissue heterogeneity and the complexity of light propagation through multiple layers of tissue [34-36], any variability in adipose thickness will affect the measurement sensitivity on muscle oxygenation and limit the accuracy of inter-subject comparison [16, 37]. Furthermore, errors can be introduced by assuming constant tissue scattering, which is typically required in CW-NIRS. For example, Hammer et al. performed a vascular occlusion test using a 250 mmHg inflated tourniquet on the brachial artery of human subjects and demonstrated when scattering was assumed to be constant, changes in tissue oxygenation were overestimated [20]. This may have an important clinical impact in orthopaedic surgery since NIRS calculated deoxygenation and reoxygenation rates have been previously used to describe muscle oxidative injury due to tourniquet application [9]. Quantifying incorrect oxygen changes may lead to an inaccurate understanding of tourniquet induced muscle damage. Thus, it is important to use a quantitative broadband DOS technique to correctly calculate and correct for the effects of optical scattering in order to represent accurate hemodynamics based on patient specific tissue composition.

Our findings show no significant relationship between the following baseline hemoglobin parameters and $W/L - StO_2$, HbO_2 , HbR . We report a low W/L ratio seen in most subjects, representing an increased amount of adipose in the interrogated tissue. Nevertheless, the subcutaneous layer contains vasculature sensitive to regional

hemodynamics and therefore, we were able to assess tissue metabolism using DOS with the linear rate of deoxygenation and $tMRO_2$. $tMRO_2$ was calculated using methods previously described [38, 39]. Our results for $tMRO_2$ are similar to those presented by Wang et al., where the reported metabolic activity in adipose tissue was determined to be $0.5 \mu M/sec$ [40]. Since most of our subjects had a relatively low W/L, metabolic activity reflecting adipose tissue is expected [41]. Breakpoint StO_2 , as we defined it, has been used previously to describe the extent of ischemia and the point where oxygen consumption and delivery is at equilibrium [32, 33]. It should be recognized that our findings of $\sim 40\%$ oxygen saturation “plateau”, which we defined as breakpoint StO_2 agrees with what has been previously reported in the literature for arterial occlusions greater than 200 mmHg of the brachioradialis [42]. This study did not report the source-detector separation or whether a multi-layer correction factor was used [42]. However, it was mentioned that a quantitative NIRS technique was employed [42]. In our study, we did not observe a correlation between W/L and breakpoint StO_2 , as it did not differ between groups.

A hemodynamic hyperemic response (HHR) following tourniquet deflation was observed in 18 of 24 subjects. The HHR may reflect a healthy, reactive endothelial response to tissue ischemia and the dramatic increase in blood flow following tourniquet release [43]. Similarly, the time it takes to reach post-occlusive StO_2 max, defined as T_{peak} may be an index of microvascular function [43]. There was no correlation observed between the total tourniquet time and hemodynamic parameters during reperfusion. Previously, Tujar et al. used NIRS to show that microvascular compliance, as indicated by changes in StO_2 following tourniquet release, decreases after 90 minutes of tourniquet

induced ischemia in subjects' undergoing hand surgery [10]. It was suggested that significant changes in reperfusion parameters occurred after 90 minutes of tourniquet induced ischemia [10]. Although these findings were not observed in our study, it may be because we only had four subjects with tourniquet times greater than 90 minutes. In our study, our multivariable analysis indicated a negative correlation between subjects' pre-inflation baseline StO_2 and HHR following tourniquet release. This suggests that pre-inflation tissue oxygenation as measured by DOS may be able to predict the range of expected values and extent of the magnitude for the post-occlusive hyperemic response. Similarly, Lin et al. reported that twenty-six subjects undergoing tourniquet assisted ankle surgery exhibited a strong negative correlation between their baseline NIRS tissue oxygen levels and the hyperemic magnitude after tourniquet release [8]. The relationship between HHR and T_{peak} with W/L was not significant. Interestingly, subjects with a high W/L ratio exhibited greater dynamic changes in lipid during deoxygenation and reperfusion. This is likely due to high W/L subjects having smaller lipid concentration and thus, greater discernable changes during deoxygenation and reperfusion as compared to subjects with higher lipid concentration.

There were several limitations to this study. First, this study was designed as a pilot study to assess the feasibility of DOS in this intraoperative application. As such, the study had a limited sample size and was underpowered to assess differences between high and low W/L groups. Second, clinical outcomes such as post-operative pain, edema and strength were not investigated and clinical parameters such as smoking status and intraoperative blood pressure were not obtained. Third, due to limited intraoperative experience with DOS on lower extremity soft tissues, SNR was insufficient in 5 of the

excluded subjects. With low SNR, DOS fails to separate absorption from scattering in highly attenuated, ischemic tissue resulting in poor data quality. Finally, our subject dependent W/L ratios were not validated with ultrasound. Thus, W/L was only used to estimate the measured levels of lean tissue compared to adipose.

In conclusion, we show that broadband DOS can be used intraoperatively to measure real-time soft tissue hemodynamics distal to a tourniquet on the lower extremity and established the range of hemodynamics during tourniquet use. In addition, we obtained robust physiological information on tissue metabolism using a linear piecewise fit during the deoxygenation phase of a long duration tourniquet induced occlusion. Moreover, the use of DOS calculated water and lipid fractions enabled us to determine hemodynamic parameters that are both dependent and independent of W/L ratios. Although the clinical application of this technology is still investigational, our findings are supportive of previous reports in the literature relating to noninvasive monitoring of tissue hemodynamics during tourniquet assisted orthopaedic surgeries. With additional studies, we believe DOS may serve as a viable research tool to better understand how tourniquet use is related to post-operative outcomes, and therefore inform and optimize tourniquet usage in this and other surgical applications. Finally, the importance of using DOS in these clinical applications may increase the understanding and improve the validity of hemodynamic changes observed when comparing highly variable, patient-specific differences in tissue composition.

Acknowledgements:

This research was supported by the Laser Microbeam and Medical Program (LAMMP, NIH P41EB015890), an NIH TL-1 training fellowship (NIH 8UL1TR000153), an NIH

CTSA grant (NIH UL1 TR000153), and a DOD Breast Cancer Research Program postdoctoral fellowship (W81XWH-13-1-0001). Additional support was also provided by the Arnold and Mabel Beckman Foundation.

References:

1. Abdel-Salam, A. and K.S. Eyres, *Effects of tourniquet during total knee arthroplasty. A prospective randomised study.* J Bone Joint Surg Br, 1995. **77**(2): p. 250-3.
2. Jiang, F.Z., H.M. Zhong, Y.C. Hong, and G.F. Zhao, *Use of a tourniquet in total knee arthroplasty: a systematic review and meta-analysis of randomized controlled trials.* J Orthop Sci, 2015. **20**(1): p. 110-23.
3. Wakankar, H.M., J.E. Nicholl, R. Koka, and J.C. D'Arcy, *The tourniquet in total knee arthroplasty. A prospective, randomised study.* J Bone Joint Surg Br, 1999. **81**(1): p. 30-3.
4. Huang, Z.Y., F.X. Pei, J. Ma, et al., *Comparison of three different tourniquet application strategies for minimally invasive total knee arthroplasty: a prospective non-randomized clinical trial.* Arch Orthop Trauma Surg, 2014. **134**(4): p. 561-70.
5. Li, X., L. Yin, Z.Y. Chen, et al., *The effect of tourniquet use in total knee arthroplasty: grading the evidence through an updated meta-analysis of randomized, controlled trials.* Eur J Orthop Surg Traumatol, 2014. **24**(6): p. 973-86.

6. Zhang, W., N. Li, S. Chen, et al., *The effects of a tourniquet used in total knee arthroplasty: a meta-analysis*. J Orthop Surg Res, 2014. **9**(1): p. 13.
7. Estebe, J.P., J.M. Davies, and P. Richebe, *The pneumatic tourniquet: mechanical, ischaemia-reperfusion and systemic effects*. Eur J Anaesthesiol, 2011. **28**(6): p. 404-11.
8. Lin, L., G. Li, J. Li, and L. Meng, *Tourniquet-induced tissue hypoxia characterized by near-infrared spectroscopy during ankle surgery: an observational study*. BMC Anesthesiol, 2019. **19**(1): p. 70.
9. Shadgan, B., W.D. Reid, R.L. Harris, et al., *Hemodynamic and oxidative mechanisms of tourniquet-induced muscle injury: near-infrared spectroscopy for the orthopedics setting*. J Biomed Opt, 2012. **17**(8): p. 081408-1.
10. Tujjar, O., A.R. De Gaudio, L. Tofani, and A. Di Filippo, *Effects of prolonged ischemia on human skeletal muscle microcirculation as assessed by near-infrared spectroscopy*. J Clin Monit Comput, 2017. **31**(3): p. 581-588.
11. Ferrari, M., L. Mottola, and V. Quaresima, *Principles, techniques, and limitations of near infrared spectroscopy*. Can J Appl Physiol, 2004. **29**(4): p. 463-87.
12. Wahr, J.A., K.K. Tremper, S. Samra, and D.T. Delpy, *Near-Infrared spectroscopy: Theory and applications*. Journal of Cardiothoracic and Vascular Anesthesia, 1996. **10**(3): p. 406-418.
13. Geraskin, D., H. Boeth, and M. Kohl-Bareis, *Optical measurement of adipose tissue thickness and comparison with ultrasound, magnetic resonance imaging, and callipers*. J Biomed Opt, 2009. **14**(4): p. 044017.

14. Niwayama, M., L. Lin, J. Shao, et al., *Quantitative measurement of muscle hemoglobin oxygenation using near-infrared spectroscopy with correction for the influence of a subcutaneous fat layer*. Review of Scientific Instruments, 2000. **71**(12): p. 4571-4575.
15. Ohmae, E., S. Nishio, M. Oda, et al., *Sensitivity correction for the influence of the fat layer on muscle oxygenation and estimation of fat thickness by time-resolved spectroscopy*. J Biomed Opt, 2014. **19**(6): p. 067005.
16. van Beekvelt, M.C., M.S. Borghuis, B.G. van Engelen, et al., *Adipose tissue thickness affects in vivo quantitative near-IR spectroscopy in human skeletal muscle*. Clin Sci (Lond), 2001. **101**(1): p. 21-8.
17. Bevilacqua, F., A.J. Berger, A.E. Cerussi, et al., *Broadband absorption spectroscopy in turbid media by combined frequency-domain and steady-state methods*. Appl Opt, 2000. **39**(34): p. 6498-507.
18. Cerussi, A., N. Shah, D. Hsiang, et al., *In vivo absorption, scattering, and physiologic properties of 58 malignant breast tumors determined by broadband diffuse optical spectroscopy*. J Biomed Opt, 2006. **11**(4): p. 044005.
19. O'Sullivan, T., A. Cerussi, B. Tromberg, and D. Cuccia, *Diffuse optical imaging using spatially and temporally modulated light*. Journal of Biomedical Optics, 2012. **17**(7): p. 071311.
20. Hammer, S.M., D.M. Hueber, D.K. Townsend, et al., *Effect of assuming constant tissue scattering on measured tissue oxygenation values during tissue ischemia and vascular reperfusion*. Journal of Applied Physiology, 2019. **127**(1): p. 22-30.

21. Gramatikov, B., "*Handbook of biomedical optics*", edited by David A. Boas, Constantinos Pitris, and Nimmi Ramanujam. BioMedical Engineering OnLine, 2012. **11**(1): p. 7.
22. Lee, J., J.G. Kim, S. Mahon, et al., *Tissue hemoglobin monitoring of progressive central hypovolemia in humans using broadband diffuse optical spectroscopy*. Journal of Biomedical Optics, 2008. **13**(6): p. 064027.
23. Tromberg, B.J., N. Shah, R. Lanning, et al., *Non-invasive in vivo characterization of breast tumors using photon migration spectroscopy*. Neoplasia, 2000. **2**(1-2): p. 26-40.
24. Cerussi, A., D. Hsiang, N. Shah, et al., *Predicting response to breast cancer neoadjuvant chemotherapy using diffuse optical spectroscopy*. Proc Natl Acad Sci U S A, 2007. **104**(10): p. 4014-9.
25. O'Sullivan, T.D., A. Leproux, J.H. Chen, et al., *Optical imaging correlates with magnetic resonance imaging breast density and reveals composition changes during neoadjuvant chemotherapy*. Breast Cancer Res, 2013. **15**(1): p. R14.
26. Warren, R.V., J. Cotter, G. Ganesan, et al., *Noninvasive optical imaging of resistance training adaptations in human muscle*. J Biomed Opt, 2017. **22**(12): p. 1-9.
27. Kam, P.C.A., R. Kavanaugh, and F.F.Y. Yoong, *The arterial tourniquet: pathophysiological consequences and anaesthetic implications*. Anaesthesia, 2001. **56**(6): p. 534-545.

28. Kumar, K., C. Railton, and Q. Tawfic, *Tourniquet application during anesthesia: "What we need to know?"*. Journal of anaesthesiology, clinical pharmacology, 2016. **32**(4): p. 424-430.
29. Saied, A., A. Ayatollahi Mousavi, F. Arabnejad, and A. Ahmadzadeh Heshmati, *Tourniquet in surgery of the limbs: a review of history, types and complications*. Iranian Red Crescent medical journal, 2015. **17**(2): p. e9588-e9588.
30. Brooksby, B., B.W. Pogue, S. Jiang, et al., *Imaging breast adipose and fibroglandular tissue molecular signatures by using hybrid MRI-guided near-infrared spectral tomography*. Proc Natl Acad Sci U S A, 2006. **103**(23): p. 8828-33.
31. Ganesan, G., J.A. Cotter, W. Reuland, et al., *Effect of blood flow restriction on tissue oxygenation during knee extension*. Med Sci Sports Exerc, 2015. **47**(1): p. 185-93.
32. Carreau, A., B. El Hafny-Rahbi, A. Matejuk, et al., *Why is the partial oxygen pressure of human tissues a crucial parameter? Small molecules and hypoxia*. J Cell Mol Med, 2011. **15**(6): p. 1239-53.
33. Collins, J.A., A. Rudenski, J. Gibson, et al., *Relating oxygen partial pressure, saturation and content: the haemoglobin-oxygen dissociation curve*. Breathe (Sheff), 2015. **11**(3): p. 194-201.
34. Creteur, J., A.P. Neves, and J.L. Vincent, *Near-infrared spectroscopy technique to evaluate the effects of red blood cell transfusion on tissue oxygenation*. Crit Care, 2009. **13** Suppl 5(Suppl 5): p. S11.

35. Delpy, D.T. and M. Cope, *Quantification in tissue near-infrared spectroscopy*. Philosophical Transactions of the Royal Society B: Biological Sciences, 1997. **352**(1354): p. 649-659.
36. Pucci, O., S. Sharieh, and V. Toronov, *Spectral and spatial characteristics of the differential pathlengths in non-homogeneous tissues*. SPIE BiOS. Vol. 6855. 2008: SPIE.
37. Homma, S., T. Fukunaga, and A. Kagaya, *Influence of adipose tissue thickness on near infrared spectroscopic signal in the measurement of human muscle*. Journal of Biomedical Optics, 1996. **1**(4).
38. Boas, D.A. and M.A. Franceschini, *Haemoglobin oxygen saturation as a biomarker: the problem and a solution*. Philosophical transactions. Series A, Mathematical, physical, and engineering sciences, 2011. **369**(1955): p. 4407-4424.
39. Ghijssen, M., G.R. Lentsch, S. Gioux, et al., *Quantitative real-time optical imaging of the tissue metabolic rate of oxygen consumption*. J Biomed Opt, 2018. **23**(3): p. 1-12.
40. Wang, Z., Z. Ying, A. Bosy-Westphal, et al., *Evaluation of specific metabolic rates of major organs and tissues: comparison between men and women*. Am J Hum Biol, 2011. **23**(3): p. 333-8.
41. Gerovasili, V., S. Dimopoulos, G. Tzanis, et al., *Utilizing the vascular occlusion technique with NIRS technology*. International Journal of Industrial Ergonomics, 2010. **40**(2): p. 218-222.

42. Bigio, I.J. and S. Fantini, *Quantitative biomedical optics: theory, methods, and applications*. 2016: Cambridge University Press.
43. Shirazi, B.R., R.J. Valentine, and J.A. Lang, *Reproducibility and normalization of reactive hyperemia using laser speckle contrast imaging*. PLOS ONE, 2021. **16**(1): p. e0244795.

Figure legends:

Figure 1. A) Fiber coupled DOS sensor probe placed distal to the tourniquet. B) Probe secured using adhesive tape to ensure contact with skin. C) Sterile drapes placed distal to the probe to ensure a sterile operating field (proximal part of the limb is at the top of the images and the distal leg and knee are at the bottom). DOS = diffuse optical spectroscopy.

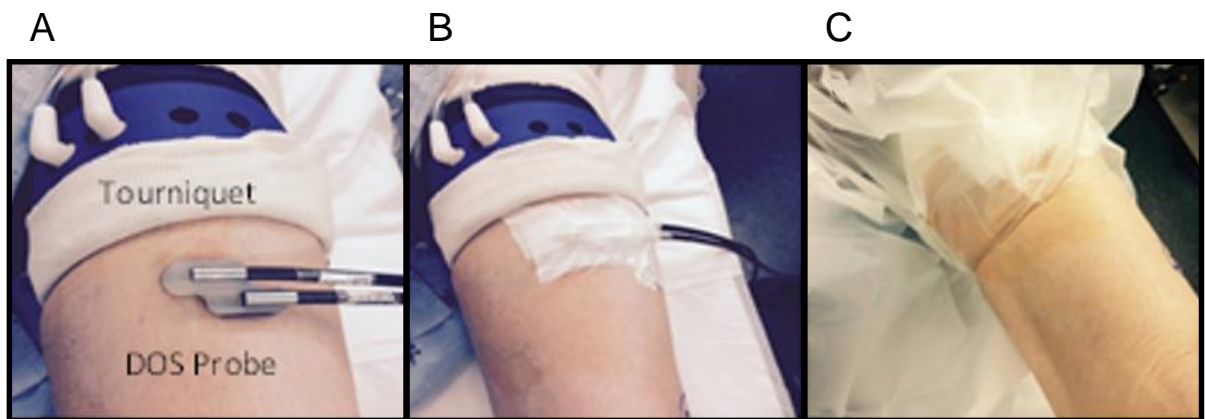
Figure 2. Fitting metrics used for analysis shown for a representative case: a) StO_2 dynamics with a linear piecewise fit used to determine breakpoint between rapid deoxygenation phase and steady state ischemia and b) $tMRO_2$ represented by the slope of a linear regression fit between 0.5 minutes and the time at breakpoint. Time is shown after tourniquet inflation. StO_2 = somatic tissue oxygen saturation; $tMRO_2$ = tissue metabolic rate of oxygenation.

Figure 3. DOS parameter changes of StO_2 (a), HbO_2 (b), HbR (c), THb (d), water fraction (e), lipid fraction (f), and W/L ratio (g) during deoxygenation within high (line color - blue) and low (line color - red) W/L Ratio groups. Data at each time point represents an average (+/- 15 secs). DOS = diffuse optical spectroscopy; StO_2 = somatic tissue oxygen saturation; HbO_2 = oxyhemoglobin; HbR = deoxyhemoglobin; THb = Total Hemoglobin; W/L = Water/Lipid.

Figure 4. Relationships observed between baseline StO₂ (a) and baseline THb (b) with the subjects' hemodynamic hyperemic response (HHR). StO₂ = somatic tissue oxygen saturation; THb = Total Hemoglobin; HHR = hemodynamic hyperemic response.

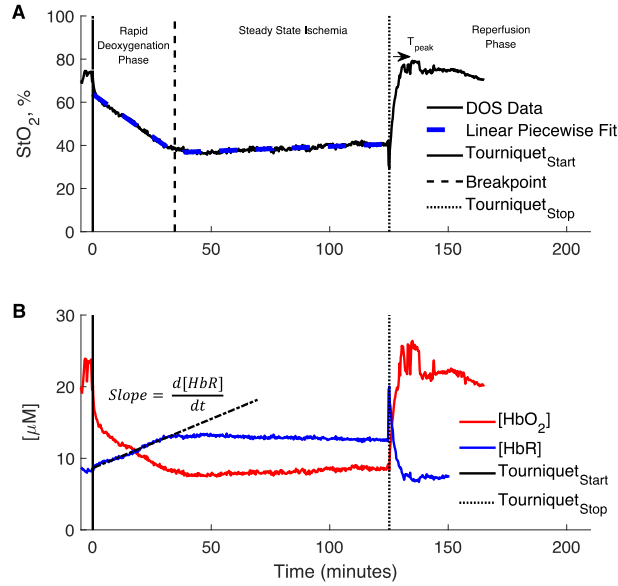
Figure 5. DOS parameter changes of StO₂ (a), HbO₂ (b), HbR (c), THb (d), water fraction (e), lipid fraction (f), and W/L ratio (g) during reperfusion within high (line color - blue) and low (line color - red) W/L Ratio groups. Data at each time point represents an average (+/- 15 secs). DOS = diffuse optical spectroscopy; StO₂ = somatic tissue oxygen saturation; HbO₂ = oxyhemoglobin; HbR = deoxyhemoglobin; THb = Total Hemoglobin; W/L = Water/Lipid.

Figure 1



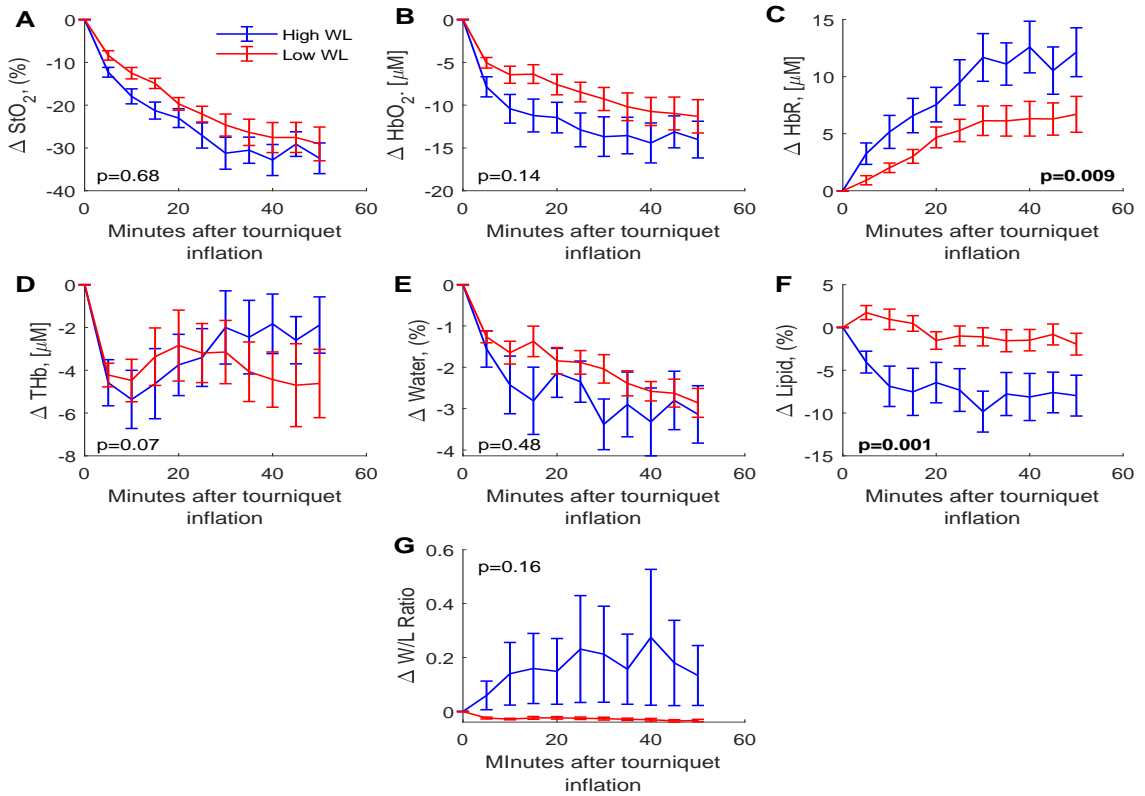
56.3 mm x 160.8 mm

Figure 2



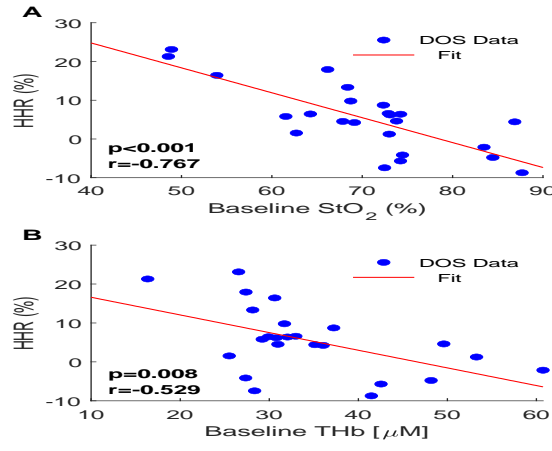
78.5 mm x 81.3 mm

Figure 3



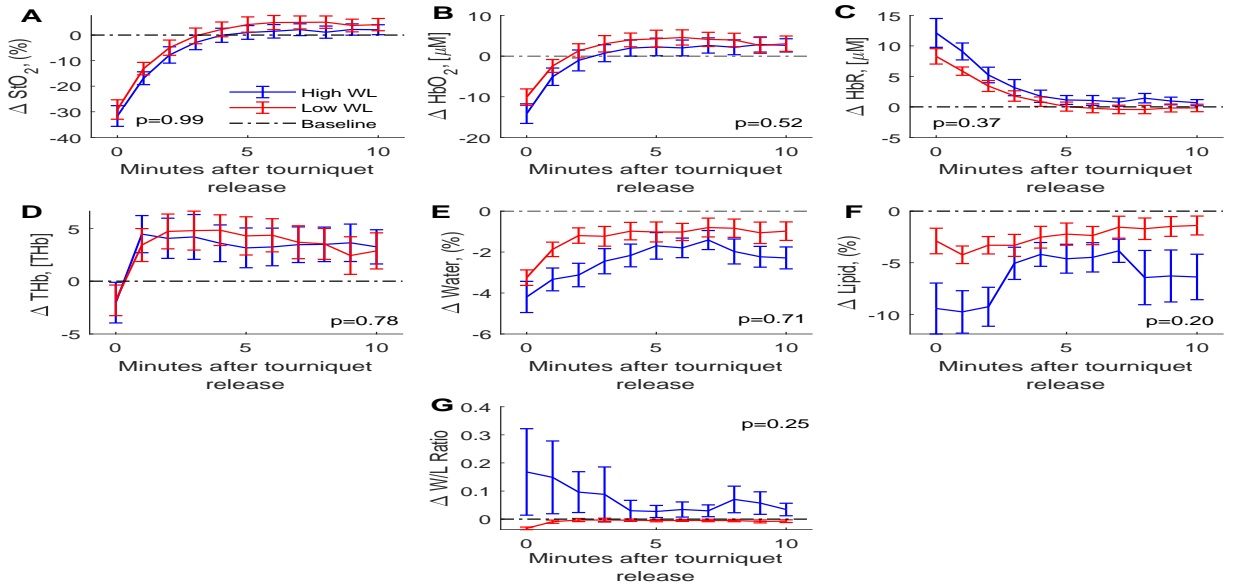
137.2 mm x 150.6 mm

Figure 4



117.9 mm x 75.9 mm

Figure 5



137.2 mm x 163.2 mm

Table 1. Tourniquet time and subject characteristics (Age, BMI, Height, Weight, Ethnicity, Gender, and Comorbidities) for all subjects analyzed. SD = Standard Deviation; BMI = Body Mass Index; W/L = Water/Lipid.

Parameters	All subjects (n=24)_	Low W/L (n=12)	High W/L (n=12)	Range
Tourniquet Total Time, min	78.7 ± 16.9 (mean ± SD)	75.8 ± 16.8	81.6 ± 17.2	57.3 – 125.1
Age, yrs	63.5 ± 12.5 (mean ± SD)	65.3 ± 15.8	61.7 ± 8.4	25 – 82
BMI, kg/m ²	30.5 ± 6.7 (mean ± SD)	32.5 ± 7.3	28.4 ± 5.8	15.6 – 41.7
Height, cm	170.8 ± 11.2 (mean ± SD)	165.0 ± 8.3	175.9 ± 11.2	154.9 - 193
Weight, kg	88.5 ± 20.7 (mean ± SD)	89.4 ± 24.0	87.0 ± 17.8	38.6 - 124
Ethnicity, n				
Caucasian	n=17	n=7	n=10	
Asian	n=1	n=1	n=0	
Hispanic	n=6	n=4	n=2	
Gender, n				
Male	n=11	n=3	n=8	
Female	n=13	n=9	n=4	
Comorbidities, n				
None	n=9	n=4	n=5	
Rheumatoid Arthritis	n=1	n=1	n=0	
Hyperlipidemia	n=7	n=3	n=4	
Hypertension	n=9	n=5	n=4	
Hypothyroidism	n=4	n=2	n=2	
Iron deficiency anemia	n=1	n=0	n=1	
Pernicious anemia	n=1	n=0	n=1	
Systemic Lupus Erythematosus	n=1	n=1	n=0	
Antiphospholipid syndrome	n=1	n=1	n=0	
Diabetes Mellitus type 2	n=4	n=2	n=2	
Multiple Sclerosis	n=1	n=0	n=1	
Coronary Artery Disease	n=1	n=0	n=1	

Table 2. Summary of linear regression analysis for correlation between baseline hemodynamic parameters and baseline W/L in all subjects. W/L = Water/Lipid; StO₂ = Somatic tissue oxygen saturation; HbO₂ = Oxyhemoglobin; HbR = Deoxyhemoglobin; THb = Total Hemoglobin

DOS Hemodynamic Parameters	r	P-value
StO ₂ , %	0.11	0.61
HbO ₂ , [μM]	0.39	0.06
HbR, [μM]	0.29	0.18
THb, [μM]	0.46	0.02

Table 3. Multivariable regression for hemodynamic outcomes predicted by W/L ratio and subject characteristics (gender, age, BMI, Baseline StO₂, Baseline THb). Bold indicates significance (p<0.05). CI = confidence interval; W/L = Water/Lipid; BMI = Body Mass Index; StO₂ = Somatic tissue oxygen saturation; THb = Total Hemoglobin.

	First Phase Duration (min)	Linear Rate of Deoxygenation (%/min)	tMRO ₂ ([μM]/sec)	Breakpoint StO ₂	HHR (%)	T _{peak} (min)
W/L Ratio						
β-coefficient	-11.6	-1.9	0.7	-3.7	-0.3	0.08
95% CI	-30.6,7.4	-2.6,-1.3	0.2,1.2	-24.2,16.9	-13.0,12.4	-4.7,4.9
p-value	0.22	<0.0001	0.008	0.71	0.96	0.97
Female						
β-coefficient	2.2	-0.04	-0.1	-3.0	1.6	-1.1
95% CI	-6.6,11.0	-0.4,0.3	-0.3,0.1	-12.6,6.5	-4.3,7.5	-3.5,1.3
p-value	0.60	0.80	0.29	0.51	0.57	0.34
Age						

β -coefficient	-0.06	-0.001	-0.001	0.07	0.05	0.05
95% CI	-0.4,0.3	-0.01,0.01	-0.01,0.008	-0.3,0.5	-0.2,0.3	-0.04,0.15
p-value	0.71	0.87	0.82	0.73	0.65	0.27
BMI						
β -coefficient	0.21	0.02	-0.01	0.12	-0.16	-0.05
95% CI	-0.5,0.9	-0.009,0.04	-0.03,0.007	-0.7,0.9	-0.6,0.3	-0.23,0.13
p-value	0.54	0.18	0.22	0.75	0.50	0.60
Baseline StO₂						
β -coefficient	1.2	0.2	-0.0007	-0.1	-0.66	0.07
95% CI	0.6,1.8	0.0003,0.04	-0.02,0.01	-0.7,0.5	-1.04,-0.3	-0.09,0.2
p-value	<0.001	0.05	0.92	0.75	0.002	0.36
Baseline THb						
β -coefficient	-0.6	-0.02	0.01	0.3	-0.03	0.009
95% CI	-1.3,0.05	-0.05,0.002	0.005,0.03	-0.5,1.0	-0.5,0.4	-0.18,0.2
p-value	0.06	0.06	0.15	0.4	0.9	0.93